SINGULARLY PERTURBED ORDINARY DIFFERENTIAL EQUATIONS WITH TIME DELAY AND ADVANCED SHIFTS

A Thesis Submitted
in Partial Fulfillment of the Requirements for the
Degree of

MASTER OF SCIENCE

in

MATHEMATICS

by

Divyanshi Dasila
Roll No. 24/MScMAT/41

Shirsthi Kaushik
Roll No. 24/MScMAT/42

Under the Supervision of

Prof. Aditya Kaushik

Department of Applied Mathematics
Delhi Technological University

DEPARTMENT OF APPLIED MATHEMATICS
DELHI TECHNOLOGICAL UNIVERSITY
Shahbad Daulatpur, Main Bawana Road, Delhi – 110042, India

May 2025

DELHI TECHNOLOGICAL UNIVERSITY

(Formerly Delhi College of Engineering)

Shahbad Daulatpur, Main Bawana Road, Delhi – 110042, India

CANDIDATE'S DECLARATION

We, **Divyanshi Dasila (24/MScMAT/41)** and **Shirsthi Kaushik (24/MScMAT/42)**, hereby declare that the work presented in this thesis entitled **SINGULARLY PERTURBED ORDINARY DIFFERENTIAL EQUATIONS WITH TIME DELAY AND ADVANCED SHIFTS** is an authentic record of our own study carried out during the period from **August 2025 to May 2026** under the supervision of **Prof. Aditya Kaushik**, Department of Applied Mathematics, Delhi Technological University.

The material presented in this report has not been submitted by us for the award of any other degree of this or any other institute.

Candidate's Signature **Candidate's Signature**

This is to certify that the students have incorporated all corrections suggested during evaluation, and the statement made by the candidates is to the best of our knowledge.

Signature of Supervisor **Signature of External Examiner**

DELHI TECHNOLOGICAL UNIVERSITY

(Formerly Delhi College of Engineering)
Shahbad Daulatpur, Main Bawana Road, Delhi – 110042, India

CERTIFICATE

This is to certify that **Divyanshi Dasila (24/MScMAT/41)** and **Shirsthi Kaushik (24/MScMAT/42)** have successfully completed the thesis entitled **SINGULARLY PERTURBED ORDINARY DIFFERENTIAL EQUATIONS WITH TIME DELAY AND ADVANCED SHIFTS** as part of their academic requirements in the Department of Applied Mathematics, Delhi Technological University, Delhi.

The work presented in this thesis has been carried out under my supervision. To the best of my knowledge, this thesis is a bona fide record of the student's effort and has not been submitted to any other institution for any academic purpose.

Signature

(Prof. Aditya Kaushik)
Department of Applied Mathematics

Contents

Abstract

Differential equations play a fundamental role in modelling real-world phenomena in science and engineering. The class of problems called singularly perturbed differential problems had a major role in setting up the foundations of fluid dynamics, control theleads to turning-point. The presence of sharp boundaries or interior layers can be observed in the solutions due to the multiplication of the highest order derivative by a small perturbation parameter called ε. The introduction of other parameters, such as delay, advanced, or a combination of both, makes the problem harder to solve. Furthermore, the vanishing of the convection term leads to turning-point problems and interior layers, making the problem more challenging. In this thesis, we study a class of singularly perturbed differential-difference equations with mixed delay and advance. We study two cases with respect to delays and advances of order $o(\varepsilon)$ and $O(\varepsilon)$. Numerical results and applications are presented to confirm the theoretical analysis and also show how the delay and advance terms affect the position of the interior layer, while the rate of convergence does not depend on the perturbation and shift parameters.

Chapter 1

Introduction

Differential equations play a fundamental role in modelling real-world phenomena in science and engineering. Many physical systems involve processes that occur on multiple scales. By relating a variable's rate of change to the variable itself, they enable us to analyze and predict the behaviour of the model over time and space. Their versatility makes them indispensable in scientific and technological fields [22, 25].
Not all differential equations are easily solvable. Some differential equations do not provide exact solutions. Thus, we must use mathematical methods to find approximate solutions to complex, unsolvable problems that depend on a small parameter ε, based on exact solutions of simple, related systems. This theory is called **Perturbation Theory**, and the differential equations or problems we work on are called **Perturbation Problems** [21, 25]. Generally, the equation is considered as

$$D_\varepsilon : \varepsilon u''(x) + a(x)u'(x) + b(x)u(x) = 0, \tag{1.1}$$

where ε is a small parameter.

Types of Perturbation Problems

We classify them as:

1. Regularly Perturbed Problems
2. Singularly Perturbed Problems

As we are focusing on a singularly perturbed differential equation, we will discuss it only.

1.1 Singular Perturbation Problems

Singular perturbation problems involve a small parameter ε multiplying the highest-order derivative term. In such problems, even a small change can lead to a major change in the solution's behavior.

The general form of a singularly perturbed boundary value problem is

$$\varepsilon y''(x) + a(x)y'(x) + b(x)y(x) = f(x), \qquad 0 < x < 1 \tag{1.2}$$

subject to the presecribed boundary conditions [21, 25]

$$y(0) = \alpha, \qquad y(1) = \beta \tag{1.3}$$

where ε is a small positive perturbation parameter and $a(x)$, $b(x)$, and $f(x)$ are smooth functions.

The behavior of the solution depends upon the perturbation parameter ε. As ε approaches zero, the highest order derivative term in the equation disappears, and the equation reduces to a lower form [18, 25]

$$a(x)y'(x) + b(x)y(x) = f(x) \tag{1.4}$$

The reduced equation generally does not satisfy both boundary conditions simultaneously because the original problem is of higher order. As a consequence, narrow regions with rapid solution variation may develop. These regions are classified as boundary layers and interior layers [18, 25]. Boundary layers occur near one or both boundaries of the domain and are characterized by abrupt changes in the solution over a short interval, whereas outside these regions the solution remains comparatively smooth. Interior layers usually arise near turning points where the convection coefficient changes sign or becomes zero.

Within layer regions, solutions may attain large values as the parameter decreases. This behavior introduces analytical and computational difficulties, as classical numerical schemes often fail to capture steep gradients accurately without specialized techniques [18, 25].

Depending on the coefficients $a(x)$ and $b(x)$, singular perturbation problem may be categorized as: [25]

- **reaction-diffusion problem** : $a(x) = 0$ and $b(x) \neq 0$,
- **convection–diffusion problem** : $b(x) = 0$ and $a(x) \neq 0$.

0

1.1.1 Applications of Singular Perturbation Problems

Singular perturbation problems arise in many scientific and engineering applications. Such models are used in situations involving diffusion, convection, reaction mechanisms, transport phenomena, and rapid transition processes [25].

In fluid mechanics and dynamics, these models are used to analyze viscous flows and boundary-layer phenomena. They are also widely used in aerodynamics, combustion theory, plasma dynamics, rarefied gas dynamics, and magneto-hydrodynamics [4, 25].

Convection-diffusion equations are used to simulate convective heat transfer systems with high Peclet numbers.Reaction-diffusion models are used in chemical reactor theory and nuclear engineering problems [21, 25].

Applications also arise in semiconductor modeling, particularly in the context of drift-diffusion equations used to model carrier transport. In areas such as control theory and oceanography, these problems provide a frame for studying transport processes on multiple scales. [25].

1.1.2 Singularly Perturbed Differential-Difference Equations

Singularly perturbed differential-difference equations (SPDDEs) extend singular perturbation models by adding shifted arguments with the small perturbation parameter. The shifted arguments represent delayed or future states of the system.

A general representation of an SPDDE is [1, 7]

$$\varepsilon y''(x) + a(x)y'(x) - b(x)y(x) + c(x)y(x-\delta) + d(x)y(x+\eta) = f(x) \tag{1.5}$$

where δ and η denote delay and advance parameters, respectively.

The model includes terms of the form $y(x-\delta)$, advanced interaction through $y(x+\eta)$, or combinations of both. In some situations, turning point problems arise when the convection coefficient $a(x)$ changes sign or vanishes at an interior point of the domain, resulting in interior layer behavior [2, 6, 26].

Such equations appear in many practical fields, including control theory, physiological processes, biological systems, neural networks, semiconductor theory, and signal transmission [1, 7, 19, 20].

Turning point problems are particularly important because the solution behavior changes rapidly near points where the convection coefficient $a(x)$ vanishes.

Because layers are present within the domain rather than at the boundaries, turning-point problems are difficult to solve numerically [2, 26].

1.1.3 Motivation of the Present Work

The present study is motivated by applications of singularly perturbed differential-difference equations in neuronal activity and synaptic signal transmission [28, 29].

In neurophysiological systems, the generation of action may be influenced by delayed responses and interactions occurring over different time scales. Such effects can be represented mathematically by differential–difference equations that include both delay and advance terms. A representative mathematical model describing the expected first-exit time associated with membrane potential dynamics is given in [29]

$$\frac{\sigma^2}{2}u''(x) + (\mu - x)u'(x) + \lambda_e u(x + a_e) + \lambda_i u(x - a_i) - (\lambda_e + \lambda_i)u(x) = -1 \tag{1.6}$$

where the membrane potential evolves under the influence of excitatory and inhibitory synaptic inputs.

The study of such models is important because many physiological and biological systems involve delayed interaction, feedback mechanisms, and rapid transitions in system behavior [8, 28, 29, 32].

Lange and Miura [16, 17] worked mostly on asymptotic analysis for non-turning point problems (a(x) = 0). Later robust numerical methods for singularly perturbed differential-difference equations with delay and advance shifts were designed by Kadalbajoo, Sharma, Patidar, Ramesh [9–12, 23] and others [26]

This drives the study toward robust and efficient parameter-uniform numerical methods for these problems, capable of handling turning points as well as delay and advance arguments.

1.1.4 Objectives of the Thesis

This thesis is devoted to the study of singularly perturbed differential-difference equations with turning point and containing delay and advance arguments.The study is composed of the theory and numerical study of these equations.

The tasks of this work are:

- Developing suitable modified numerical methods to solve singularly perturbed differential-difference equations with several perturbations.
- Studying and analyzing interior layer turning point problems.
- Accommodating advanced arguments and delaying arguments in a single numerical scheme.
- Deriving parameter-uniform estimates of the solution and its derivatives.
- Establishing convergence analysis and checking the stability of the numerical methods proposed.
- Verifying the theoretical analysis by numerically demonstrating using examples.
- Understanding the impact of shift parameters on boundary and interior layer behaviors.

The objective is to develop a uniformly convergent numerical technique whose accuracy is not affected by the perturbation parameter, even when turning points and mixed shift arguments are present.

Chapter 2

Literature Review

2.1 Introduction

As discussed in the previous chapter, singular perturbation problems are characterized by the presence of a small positive parameter ε multiplying the highest-order derivative. We had also discussed the terms boundary layers and interior layers [18, 25].

In recent decades, significant efforts have been made to develop asymptotic and numerical techniques for solving singular perturbation problems, as classical numerical methods often fail to perform adequately on uniform meshes and require a significantly large number of mesh points to achieve accurate results when the perturbation parameter is very [18, 21, 25].

The Robust numerical methods aim to obtain parameter-uniform approximations independent of the perturbation parameter. This chapter presents a detailed review of the theoretical foundations, numerical challenges, fitted numerical methods, and recent developments in the study of singularly perturbed differential equations and singularly perturbed differential-difference equations.

2.2 Foundations of Singular Perturbation Theory

The development of singular perturbation theory for differential–difference equations was significantly inspired by the pioneering work of Lange and Miura [15–17]. Their research established the way for many of the asymptotic methods that are now commonly employed in the analysis of differential-difference equations containing small perturbation parameters with delay or advance terms. Much of their work was dedicated to boundary value problems with small shifts and with strongly layered behaviour. They developed asymptotic methods able to describe the effect of arguments of delay and advance on the solution structure. The investigations were mainly confined to non-turning point problems, i.e. to the case when the convection coefficient does not become zero inside the domain, but the analytical framework introduced by them later turned out to be basic for the study of rapid oscillations and layer phenomena in singularly perturbed differential-difference equations.

With the development of singular perturbation theory, the focus slowly shifted to more complicated problems with turning points and interior layers. Turning point problems are those problems where the coefficient of the convection term changes sign in the computational domain. These problems are much more difficult to analyze because they generate interior layers instead of the normal boundary layers [2, 6, 26],. Important contributions in this direction were made by Berger, Han, and Kellogg [2], who obtained a priori estimates and numerical analysis for turning point problems. Later, Farrell [6] obtained sufficient conditions for uniform convergence of numerical schemes for singularly perturbed turning point equations.

The development of singular perturbation theory was furthur advanced through several foundational studies. Roos, Stynes, and Tobiska [25] presented a complete study on convection–diffusion and flow problems. In parallel, Miller, O'Riordan, and Shishkin [21] introduced fitted numerical techniques and

established a theoretical basis for parameter-uniform convergence in singular perturbation problems. More recent survey studies by Sharma and co-authors [26] examined the major asymptotic and numerical developments in singular perturbation theory covering the period from 1970 to 2011.

2.3 Robust Numerical Methods

Because standard numerical methods cannot accurately capture sharp boundaries or interior layers when ε is small [21, 25], specialized numerical techniques have been developed to maintain accuracy independent of ε. The specialized methods are classified into two:

2.3.1 Fitted Mesh Methods

Fitted mesh methods are constructed with specially designed non-uniform meshes where a larger number of grid points are concentrated in regions where the solution exhibits rapid variation. These layers regions are usually small in size in the computational domain, so a finer mesh is used in the neighbourhood of the layers while a coarser mesh is sufficient in the rest of the domain. Such methods can provide accurate numerical approximations with little additional computational effort by adapting the mesh according to the nature of the solution. [18, 25].

Basic Idea

Consider the problem:

$$\varepsilon u''(x) + a(x)u'(x) + b(x)u(x) = f(x), \quad 0 < x < 1, \tag{2.1}$$

subject to the boundary conditions:

$$u(0) = \alpha, \quad u(1) = \beta, \quad 0 < \varepsilon \ll 1. \tag{2.2}$$

Fitted-mesh methods have been used to solve various problems [21, 25]. The main advantage of fitted-mesh methods is that they can model layer behavior very well. At the time, they can still maintain parameter-uniform convergence. This is an advantage of the fitted mesh methods. Shishkin mesh [21] and the Bakhvalov mesh are two of the commonly used ones.

Shishkin Mesh

In Shishkin, a piecewise-uniform mesh is used, divided into fine and coarse subregions depending on the position of the boundary or interior layer. The Shishkin mesh has a transition point that changes based on the perturbation parameter ε. [21] These meshes are among the most widely used techniques for singular perturbation problems, as they have a simple structure, easy implementation. They also achieve convergence that holds across all parameters.

Bakhvalov Mesh

The Bakhvalov mesh is different from previous meshes. It uses a kind of distribution for the mesh points in a certain area. This area is called the layer region. The Bakhvalov mesh does not have a change from fine to coarse regions, unlike the Shishkin mesh. The change is smooth [3, 18].

The Bakhvalov mesh is good at showing how the exact solution behaves. This is why the Bakhvalov mesh often gives accurate numerical results. However, making the Bakhvalov mesh is more complicated mathematically.

2.3.2 Fitted Operator Methods

In fitted operator methods the computational mesh is normally kept the same over and the finite difference operator is changed instead. The main idea of these fitted operator methods is to include the way the exact solution behaves when you look at it from a distance into the discretization process so that the numerical scheme can accurately show the layer structure of the fitted operator methods [21, 27].

The fitted operator techniques [27,31] include the fitted difference method, the fitted finite volume method and the fitted Euler method. However in our work we have used the exponential fitting method [5]

In this fitting method, exponential basis functions are used to construct finite difference schemes that are similar to the exponential behavior of the exact solution inside the layer region of the exponential fitting method. Another important fitted operator method is the Il'in–Allen Southwell scheme [26,31]. This Il'in–Allen Southwell scheme introduces factors into the discretization formula to preserve the stability and monotonicity properties of the original continuous problem of the Il'in–Allen Southwell scheme. The Il'in–Allen Southwell scheme is highly effective for equations that involve both convection and diffusion and, for problems where the solution changes direction. In the work the Il'in–Allen Southwell fitting technique is used for singularly perturbed differential-difference equations when the shifts are of order $O(\varepsilon)$.

Fitted operator methods are computationally efficient because they can be implemented on uniform meshes while still providing parameter-uniform convergence. However, the construction of the fitted operator depends strongly on the analytical nature of the differential equation. [21, 27]

Chapter 3

Problem Formulation

As mentioned in Chapter 1, the singular perturbed difference-differential equation is of the form [1, 7] :

$$\varepsilon y''(x) + a(x)y'(x) - b(x)y(x) + c(x)y(x-\delta) + d(x)y(x+\eta) = f(x) \tag{3.1}$$

where δ and η denote delay and advance parameters, respectively. In this study, a family of singularly perturbed convection-diffusion equations with turning point behavior and both positive and negative changes in the reaction component is examined. Consider the boundary value problem defined on

$$\Omega = (-1, 1)$$

given by

$$L_\varepsilon y \equiv \varepsilon y''(x) + a(x)y'(x) - b(x)y(x) + c(x)y(x-\delta) + d(x)y(x+\eta) = f(x), \qquad x \in \Omega \tag{3.2}$$

subject to

$$y(x) = \phi(x), \qquad -1-\delta \le x \le -1 \tag{3.3}$$

and

$$y(x) = \gamma(x), \qquad 1 \le x \le 1+\eta \tag{3.4}$$

where the perturbation parameter is ε $(0 < \varepsilon \ll 1)$, the convection coefficient is represented by $a(x)$, the reaction coefficient is represented by $b(x)$, the delay and advance interaction strengths are represented by $c(x)$ and $d(x)$, the shift parameters are denoted by δ and η, the source function is $f(x)$, and the boundary extensions are specified by $\phi(x)$ and $\gamma(x)$ [1, 7, 15].

3.1 Turning Point Conditions

When the shifts are zero (i.e., $\delta = 0$, $\eta = 0$), the singularly perturbed differential–difference equation reduces to the corresponding ordinary differential equation. In this case, the solution exhibits either layer behavior or turning point behavior depending upon the nature of the convection coefficient $a(x)$ [25, 26].

If the convection coefficient does not change sign throughout the domain [18, 25], then the solution develops a boundary layer. The location of the layer depends on the sign of $a(x)$ over the domain $\bar{\Omega} = [-1, 1]$:

$$a(x) < 0$$

produces a left boundary layer, whereas

$$a(x) > 0$$

produces a right boundary layer.
Points within the domain where

$$a(x) = 0$$

are called turning points. At such points, the direction of convection changes, and the qualitative behavior of the solution is altered largely [2, 6].

The presence of turning points may lead to the formation of which boundary layers or interior layers in the solution. Such problems are considerably more difficult to analyze and solve numerically compared with non-turning point problems because classical numerical methods generally fail to capture the rapid variation near the turning region.

In the present study, attention is restricted to problems in which an interior layer appears in the solution. To ensure the existence of a unique turning point and exclude additional turning points inside the computational domain, the following assumptions are imposed for the equation 5.1

$$a(0) = 0, \qquad a'(0) > 0 \tag{3.5}$$

$$b(x) \geq b_0 > 0, \qquad x \in \bar{\Omega} \tag{3.6}$$

$$b(x) - c(x) - d(x) > 0, \qquad c(x) \geq 0, \qquad d(x) \geq 0, \quad x \in \bar{\Omega} \tag{3.7}$$

$$|a'(x)| \geq \frac{|a(0)|}{2}, \qquad x \in \bar{\Omega} \tag{3.8}$$

[2, 6, 26]

Condition (3.5) guarantees that the convection coefficient changes sign at the origin and therefore introduces a turning point at $x = 0$. Conditions (3.6) and (3.7) ensure positivity and stability of the reaction operator, while condition (3.8) prevents the occurrence of additional turning points within the domain.

3.2 Priori Estimates

A priori estimates establish the boundedness of the solution and its derivatives that are independent of the mesh parameters [21, 25].

We have worked on two types of shifts:

3.2.1 When it is $o(\varepsilon)$

When the shifts are sufficiently small, we use Taylor's expansion to approximate the terms containing shift arguments. Hence, we get

- For the delay term

$$y(x - \delta) = y(x) - \delta y'(x) + \frac{\delta^2}{2} y''(x) \tag{3.9}$$

- for the advance term,

$$y(x + \eta) = y(x) + \eta y'(x) + \frac{\eta^2}{2} y''(x) \tag{3.10}$$

[1,7] Substituting equations (3.9) and (3.10) into the original boundary value problem (5.1) gives the reduced singularly perturbed convection–diffusion equation

$$L_\varepsilon(u) \equiv C_\varepsilon(x)u''(x) + A_\varepsilon(x)u'(x) - B_\varepsilon(x)u(x) = f(x) \tag{3.11}$$

where

$$C_\varepsilon(x) = \varepsilon + \frac{\delta^2}{2}c(x) + \frac{\eta^2}{2}d(x) \tag{3.12}$$

$$A_\varepsilon(x) = a(x) - \delta c(x) + \eta d(x) \tag{3.13}$$

$$B_\varepsilon(x) = b(x) - c(x) - d(x) \tag{3.14}$$

[9,16] Here, $u(x)$ denotes the approximate solution obtained after replacing the shift terms by their second-order Taylor approximations.

From this analysis, we obtain the following results (lemmas) for the domain $\Omega = [-1, 1]$. (3.15)

Lemma 3.1 (Continuous Maximum Principle). [2,21]

Let $\Psi(x)$ be a sufficiently smooth function satisfying

$$\Psi(-1) \geq 0, \qquad \Psi(1) \geq 0 \tag{3.16}$$

and

$$L_\varepsilon\Psi(x) \leq 0, \qquad x \in (-1, 1) \tag{3.17}$$

where

$$L_\varepsilon\Psi = C_\varepsilon(x)\Psi''(x) + A_\varepsilon(x)\Psi'(x) - B_\varepsilon(x)\Psi(x).$$

Then,

$$\Psi(x) \geq 0, \qquad \forall x \in [-1, 1]. \tag{3.18}$$

Explanation. This lemma says that the minimum value of the solution occurs only at the boundary and not inside the domain. Further, this lemma plays an important role in the theoretical analysis of singularly perturbed differential-difference equations, as it establishes monotonicity of the solution and provides a basis for deriving stability estimates. Hence, the Continuous Maximum Principle is a fundamental analytical result used to show that the considered problem is stable and well-posed.

Lemma 3.2 (Stability Estimate). [21,25]

Let $u(x)$ be the solution of the reduced boundary value problem (3.11) together with the boundary conditions (3.15). Then,

$$\|u\| \leq \frac{\|f\|}{B_0} + \max\left(|\phi(-1)|, |\gamma(1)|\right) \tag{3.19}$$

Explanation. It states that the solution remains bounded throughout the domain and depends continuously on the forcing function $f(x)$ and the prescribed boundary conditions. Apart from boundedness, it guarantees the stability of the reduced differential operator and supports the existence and uniqueness of the solution.

3.2.2 When it is $O(\varepsilon)$

When the shifts are comparable to the perturbation parameter, the Taylor expansion approach is no longer appropriate, and the full differential-difference operator is retained.

Hence, the equation is written in the following piecewise form:

$$L_\varepsilon y \equiv \begin{cases} \varepsilon y''(x) + a(x)y'(x) - b(x)y(x) + d(x)y(x+\eta) = f(x) - c(x)\phi(x-\delta), & -1 < x \le -1+\delta \\ \varepsilon y''(x) + a(x)y'(x) - b(x)y(x) + c(x)y(x-\delta) + d(x)y(x+\eta) = f(x), & -1+\delta < x < 1-\eta \\ \varepsilon y''(x) + a(x)y'(x) - b(x)y(x) + c(x)y(x-\delta) = f(x) - d(x)\gamma(x+\eta), & 1-\eta \le x < 1 \end{cases} \tag{3.20}$$

[9,23] The piecewise formulation accounts for the fact that the shifted arguments may extend outside the computational domain near the boundaries. Therefore, the boundary extension functions $\phi(x)$ and $\gamma(x)$ are introduced. We get the following results(lemmas):

Lemma 3.3 (Minimum Principle). [2,26]

Let $\pi(x)$ be a sufficiently smooth function satisfying

$$L_\varepsilon \pi(x) \le 0, \qquad x \in \Omega \tag{3.21}$$

and

$$\pi(-1) \ge 0, \qquad \pi(1) \ge 0. \tag{3.22}$$

Then,

$$\pi(x) \ge 0, \qquad \forall x \in \bar{\Omega}. \tag{3.23}$$

Explanation.

This lemma states that if the operator L_ε does not generate if positive growth inside the domain and the boundary values remain nonnegative, then the solution cannot attain negative values in the interior of the interval. It guarantees monotonicity of the solution and sets a path for deriving stability and convergence results.

Lemma 3.4 (Stability Bound). [9,21]

Let $y(x)$ be the solution of the boundary value problem (3.20) and suppose

$$b(x) - c(x) - d(x) \ge K > 0, \qquad x \in \Omega. \tag{3.24}$$

Then,

$$|y(x)| \le \frac{\|f\|}{K} + C \max\{\|\phi\|, \|\gamma\|\} \tag{3.25}$$

where C is a positive constant independent of ε.

Explanation.

This estimate shows that the solution remains uniformly bounded and depends continuously on the forcing term and boundary extensions. The result establishes stability and ensures that perturbations in the input data do not produce uncontrolled variations in the solution.

Lemma 3.5 (Derivative Estimate). [6,26]

Assume that

$$a(x),\ b(x),\ c(x),\ d(x),\ f(x) \in C^m[-1,1]$$

and let β satisfy

$$\beta_l < \beta < \beta_s.$$

Then the solution $y(x)$ satisfies

$$|y^{(k)}(x)| \leq C\left(|x| + \sqrt{\varepsilon}\right)^{\beta-k}, \qquad k = 1, \ldots, m+1. \tag{3.26}$$

Explanation

This derivative estimate establishes parameter-uniform boundedness of the solution derivatives. It shows that even when $\varepsilon \to 0$, the growth of derivatives remains in control.It also helps to prove the convergence and robustness of the fitted numerical schemes.

3.3 Theoretical Analysis

3.3.1 Summary of A Priori Estimates

From the analysis of the two cases of a priori estimates, it is observed that for shifts of order $o(\varepsilon)$, the shifted arguments were approximated using Taylor series expansions [9,16]. This transformed the original differential–difference equation into an equivalent singularly perturbed convection–diffusion equation with modified coefficients. The theoretical analysis led to the derivation of the Continuous Maximum Principle, stability estimates, and derivative bounds. These results established positivity, boundedness, and controlled growth of derivatives near the turning point while preserving the interior layer structure.

For shifts of order $O(\varepsilon)$, the shift terms remained comparable to the diffusion parameter and therefore the complete differential–difference operator was retained [11, 23]. A piecewise formulation was introduced to incorporate boundary corrections arising due to delay and advance effects. Using the Minimum Principle, stability bounds, and derivative estimates, it was shown that the solution remains uniformly bounded and exhibits parameter-uniform regularity even in the presence of turning point behavior.

Hence, the theoretical results obtained for both shifts demonstrate that the considered singularly perturbed differential–difference problem is well posed and stable. The derived estimates set an analytical foundation for the construction, analysis, and convergence of robust numerical methods capable of accurately resolving interior layers and the effects introduced by shift parameters.

Chapter 4

Numerical Methods

4.1 Finite Difference Discretization

4.1.1 Uniform Mesh and Mesh Notation

Let the problem domain be the closed interval $\overline{\Omega} = [0, 1]$. A *uniform mesh* $\overline{\Omega}^N$ of $N+1$ equally spaced nodes is defined by

$$\overline{\Omega}^N = \big\{x_i : x_i = ih,\ i = 0, 1, \ldots, N\big\}, \qquad h = \frac{1}{N}, \tag{4.1}$$

where h is the *mesh parameter* (step size) and N is the number of subintervals. The interior and boundary point sets are denoted

$$\Omega^N = \{x_i : 1 \le i \le N-1\}, \qquad \partial\Omega^N = \{x_0, x_N\} = \{0, 1\}. \tag{4.2}$$

For a mesh function $U = \{U_i\}_{i=0}^N$ defined on $\overline{\Omega}^N$, the forward, backward, and central *difference operators* are, respectively,

$$D^+U_i = \frac{U_{i+1} - U_i}{h}, \tag{4.3}$$

$$D^-U_i = \frac{U_i - U_{i-1}}{h}, \tag{4.4}$$

$$D^0U_i = \frac{U_{i+1} - U_{i-1}}{2h}. \tag{4.5}$$

The second-order central-difference operator is

$$\delta^2U_i = D^+D^-U_i = \frac{U_{i+1} - 2U_i + U_{i-1}}{h^2}. \tag{4.6}$$

[22, 31]

4.1.2 Standard Finite Difference Approximations

Consider the general singularly perturbed two-point boundary value problem

$$\mathcal{L}u \equiv \varepsilon u''(x) + a(x)u'(x) - b(x)u(x) = f(x), \quad x \in \Omega = (0, 1), \tag{4.7}$$

with boundary conditions $u(0) = \alpha$, $u(1) = \beta$, where $0 < \varepsilon \ll 1$ is the perturbation parameter, $a(x) \ge \alpha_0 > 0$, $b(x) \ge 0$, and $f(x)$ are sufficiently smooth functions on $\overline{\Omega}$.

The *classical central-difference scheme* on $\overline{\Omega}^N$ approximates (4.7) as

$$\mathcal{L}^NU_i \equiv \varepsilon\delta^2U_i + a_iD^0U_i - b_iU_i = f_i, \quad 1 \le i \le N-1, \tag{4.8}$$

[22, 31] with $U_0 = \alpha$, $U_N = \beta$. Here $a_i = a(x_i)$, $b_i = b(x_i)$, $f_i = f(x_i)$.

The local cell-Péclet number at node x_i is

$$\mathrm{Pe}_i = \frac{|a_i|\, h}{2\varepsilon}. \tag{4.9}$$

[25, 30]

When $\mathrm{Pe}_i > 1$ the central scheme (4.8) loses its *M-matrix* property and may produce spurious oscillations [25, 30]. To recover stability uniformly in ε, fitted (exponential) schemes are required.

4.2 Exponentially Fitted Mistikawy–Werle Scheme

4.2.1 Derivation and Motivation

The *Mistikawy–Werle (MW) scheme* is an exponentially fitted finite difference scheme designed to resolve the boundary layer behaviour of the solution to (4.7) uniformly in ε. The derivation begins by seeking an exact solution of the reduced (constant-coefficient, zero-order-term) ODE on each subinterval $[x_{i-1}, x_i]$ [5].

On the mesh cell $[x_{i-1}, x_i]$, replace $a(x)$ and $b(x)$ by their mid-point values $a_{i-1/2} = a(x_{i-1/2})$ and $b_{i-1/2}$, where $x_{i-1/2} = x_{i-1} + h/2$. Consider the local problem

$$\varepsilon v'' + a_{i-1/2} v' = 0, \tag{4.10}$$

whose general solution is

$$v(x) = C_1 + C_2 \exp\Big(-\frac{a_{i-1/2}}{\varepsilon}(x - x_{i-1})\Big). \tag{4.11}$$

Enforcing $v(x_{i-1}) = U_{i-1}$ and $v(x_i) = U_i$, and differentiating, yields the *fitted first-order approximation*:

$$[\varepsilon v']_{x=x_{i-1/2}} = \frac{a_{i-1/2}\, h}{\exp(\rho_i) - 1}\Big[\exp(\rho_i) U_{i-1} - \exp(\rho_i) U_i\Big]^{\dagger}, \tag{4.12}$$

where the *fitting factor* (local Péclet number scaled argument) is

$$\rho_i = \frac{a_{i-1/2}\, h}{\varepsilon}. \tag{4.13}$$

[5, 31]

4.2.2 Fitted Operator Construction

Integrating (4.7) over the cell $[x_{i-1/2}, x_{i+1/2}]$ and applying the exponential fitting principle to the convective flux at both half-nodes leads to the *Mistikawy–Werle discrete operator*:

$$\mathcal{L}^N_{\mathrm{MW}} U_i \equiv \sigma_i^- U_{i-1} - \big(\sigma_i^- + \sigma_i^+ + b_i h\big) U_i + \sigma_i^+ U_{i+1} = h f_i, \tag{4.14}$$

for $1 \le i \le N-1$, where the left and right fitted flux coefficients are

$$\sigma_i^- = \frac{a_{i-1/2}}{\exp(\rho_i^-) - 1}, \qquad \rho_i^- = \frac{a_{i-1/2} h}{\varepsilon}, \tag{4.15}$$

$$\sigma_i^+ = \frac{a_{i+1/2}}{\exp(\rho_i^+) - 1}, \qquad \rho_i^+ = \frac{a_{i+1/2} h}{\varepsilon}. \tag{4.16}$$

[5]

4.2.3 Fitting Factors and Limiting Behaviour

The *Bernoulli function* $B(\rho) = \rho/(e^{\rho}-1)$ governs the blending between central and upwind differencing:

$$B(\rho) = \begin{cases} 1 - \dfrac{\rho}{2} + \dfrac{\rho^2}{12} - \cdots & |\rho| \ll 1, \\ \rho\, e^{-\rho}(1 + O(e^{-\rho})) & \rho \to +\infty. \end{cases} \tag{4.17}$$

[5, 27] As $\varepsilon \to 0$ (equivalently $\rho \to +\infty$), the MW scheme reduces to a first-order upwind scheme [5]. As $\varepsilon \to \infty$ (equivalently $\rho \to 0$), it recovers the standard central-difference scheme. This property makes the MW scheme *uniformly stable* across all $\varepsilon > 0$.

4.2.4 Tridiagonal System

Applying (4.14) for $i = 1, \ldots, N-1$ together with the Dirichlet conditions $U_0 = \alpha$, $U_N = \beta$ gives the $(N-1) \times (N-1)$ tridiagonal linear system

$$\mathbf{A}\,\mathbf{U} = \mathbf{F}, \tag{4.18}$$

where

$$\mathbf{A} = \begin{pmatrix} d_1 & \sigma_1^+ & & & \\ \sigma_2^- & d_2 & \sigma_2^+ & & \\ & \ddots & \ddots & \ddots & \\ & & \sigma_{N-2}^- & d_{N-2} & \sigma_{N-2}^+ \\ & & & \sigma_{N-1}^- & d_{N-1} \end{pmatrix}, \tag{4.19}$$

[21, 31] with diagonal entries $d_i = -(\sigma_i^- + \sigma_i^+ + b_i h)$ and right-hand side vector $\mathbf{F} = (hf_1 - \sigma_1^- U_0,\ hf_2,\ \ldots,\ hf_{N-2},\ hf_{N-1} - \sigma_{N-1}^+ U_N)^{\top}$. The matrix $\mathbf{A}$ is an irreducibly diagonally dominant M-matrix (because $d_i < 0$, $\sigma_i^{\pm} > 0$, and $d_i + \sigma_i^- + \sigma_i^+ \le 0$), and so there is guaranteed to be a unique solution. The problem can be solved effectively using the Thomas algorithm ($\mathcal{O}(N)$ [31]

4.3 Il'in–Allen–Southwell Fitted Scheme

4.3.1 Fitted Parameter and Upwind Discretization

The *Il'in–Allen–Southwell (IAS) scheme* [21, 27] is another widely used exponentially fitted method. It modifies the standard central-difference approximation of the first derivative by multiplying by a scalar *fitted parameter* ϕ_i chosen so that the resulting scheme is exact for solutions of a local constant-coefficient equation.

Define the upwind-weighted difference operator

$$D_{\phi}^{\mathrm{uw}} U_i = \frac{(1+\phi_i)U_{i+1} - 2U_i + (1-\phi_i)U_{i-1}}{2h}, \tag{4.20}$$

where $\phi_i \in [-1, 1]$ is the fitting parameter. The IAS scheme for (4.7) is written as

$$\mathcal{L}_{\mathrm{IAS}}^N U_i \equiv \varepsilon \delta^2 U_i + a_i D^0 U_i + a_i \phi_i D^- U_i - b_i U_i = f_i, \tag{4.21}$$

which can be rewritten in three-point form as

$$\ell_i\, U_{i-1} - m_i\, U_i + r_i\, U_{i+1} = h^2 f_i, \tag{4.22}$$

with coefficients

$$\ell_i = \varepsilon - \tfrac{a_i h}{2}(1-\phi_i), \tag{4.23}$$

$$r_i = \varepsilon + \tfrac{a_i h}{2}(1+\phi_i), \tag{4.24}$$

$$m_i = \ell_i + r_i + b_i h^2. \tag{4.25}$$

The fitting parameter is chosen by requiring that the scheme reproduces the exact solution of the reduced equation $\varepsilon v'' + a_i v' = 0$ on the local mesh cell:

$$\phi_i = \coth\!\left(\frac{a_i h}{2\varepsilon}\right) - \frac{2\varepsilon}{a_i h} = \coth(\mathrm{Pe}_i) - \frac{1}{\mathrm{Pe}_i}, \tag{4.26}$$

[21, 27]

where $\mathrm{Pe}_i = a_i h/(2\varepsilon)$ is the local Péclet number.

4.3.2 Properties of the Fitting Parameter

The function $\phi(\rho) = \coth(\rho) - 1/\rho$ (the *Langevin function*) satisfies:

1. $\phi(\rho) \in (0,1)$ for all $\rho > 0$;
2. $\phi(\rho) \to 0$ as $\rho \to 0$ (recovers central differences);
3. $\phi(\rho) \to 1$ as $\rho \to \infty$ (recovers first-order upwind differencing);
4. $\phi(\rho) = \rho/3 - \rho^3/45 + \cdots$ for small ρ.

[27]

4.3.3 Treatment Near the Turning Point

In a neighbourhood of x^* the convection coefficient changes sign, altering the direction of the boundary layer and causing the IAS fitting parameter (4.26) to become undefined (division by zero).

Regularisation at x^*. Let δ be a small parameter (typically $\delta = h^{1/2}$ or $\delta = \varepsilon^{1/2}$). Define the *modified Péclet number*

$$\widetilde{\mathrm{Pe}}_i = \frac{|a_i| h}{2\varepsilon + \delta}, \tag{4.27}$$

and replace ϕ_i in (4.26) with

$$\tilde{\phi}_i = \begin{cases} \coth(\widetilde{\mathrm{Pe}}_i) - 1/\widetilde{\mathrm{Pe}}_i & \text{if } |a_i| > \delta, \\ 0 & \text{if } |a_i| \le \delta. \end{cases} \tag{4.28}$$

This regularisation preserves the M-matrix property of $\mathbf{A}$ near x^* and maintains first-order parameter-uniform convergence [6, 26].

Special discretisation at the mesh point nearest x^*. Denoting by x_{i^*} the mesh node closest to the turning point, the coefficient a_{i^*} is evaluated using a Taylor expansion:

$$a(x) = a'(x^*)(x - x^*) + O\big((x-x^*)^2\big), \tag{4.29}$$

[2]

and the IAS scheme at i^* is replaced by the standard central-difference scheme, which is $\mathcal{O}(h^2)$ when $a \approx 0$:

$$\mathcal{L}^N_{\mathrm{CD}} U_{i^*} \equiv \varepsilon \delta^2 U_{i^*} + a_{i^*} D^0 U_{i^*} - b_{i^*} U_{i^*} = f_{i^*}. \tag{4.30}$$

[6]

4.4 Convergence Analysis

4.4.1 Parameter-Uniform Convergence: Definition

[Parameter-Uniform Convergence] A numerical method with discrete solution $\{U_i\}$ is said to be *parameter-uniformly convergent of order p* if there exists a constant C independent of both ε and N such that

$$\max_{0\le i\le N} |u(x_i) - U_i| \le C N^{-p}, \quad \forall\, \varepsilon \in (0,1],\ N \ge 1. \tag{4.31}$$

This concept, due to Miller, O'Riordan and Shishkin [21,25], is stronger than classical h-convergence because the bound (4.31) is required to hold uniformly in the perturbation parameter.

4.4.2 Main Convergence Result

Theorem 4.1 (Parameter-Uniform Convergence on Uniform Mesh)**.** *From [21, 25], let u be the exact solution of* (4.7)*, and let $\{U_i\}_{i=0}^{N}$ be the solution of either the MW scheme* (4.14) *or the IAS scheme* (4.22) *on the uniform mesh $\overline{\Omega}^N$. Then*

$$\max_{0\le i\le N} |u(x_i) - U_i| \le C\, N^{-1}, \tag{4.32}$$

where C is a positive constant independent of ε and N.

Proof. Let $e_i = u(x_i) - U_i$ be the error at node x_i. From the scheme definition, e_i satisfies

$$\mathcal{L}^N e_i = \tau_i, \quad 1 \le i \le N-1; \quad e_0 = e_N = 0. \tag{4.33}$$

Applying the discrete stability estimate (3.19) with $V = e$, boundary values zero, and using the consistency bound:

$$\|e\|_{\overline{\Omega}^N} \le C \|\tau\|_{\Omega^N} \le C \cdot C_{\text{scheme}} h = C'\, N^{-1}, \tag{4.34}$$

[21] since $h = 1/N$. The constant C' is independent of ε because both the stability constant and the consistency constant are ε-independent. □

4.4.3 Error Bounds and Sharpness

The bound (4.32) is sharp in the following sense: for the standard convection-diffusion equation with boundary layer of width $O(\varepsilon)$, the error on a uniform mesh satisfies

$$\max_i |e_i| \ge c\, \min\Big(1,\ \frac{\varepsilon}{h}\Big), \tag{4.35}$$

[25, 30] showing that classical (non-fitted) schemes exhibit $O(1)$ errors when $h \gg \varepsilon$. The fitted schemes, by contrast, achieve the uniform first-order bound (4.32) even when $h \gg \varepsilon$.

4.4.4 Theoretical Rate of Convergence

Table 4.1 summarises the theoretical convergence rates of the schemes discussed in this chapter.

Remark 4.2. On a *Shishkin mesh*, which concentrates mesh points inside the boundary layer region $[0, 2\varepsilon \ln N]$, the MW and IAS schemes achieve an improved rate of $\mathcal{O}(N^{-1} \ln N)$ Shishkin1992. On such meshes, with a second-order fitted operator, the rate can be further improved to $\mathcal{O}(N^{-2}(\ln N)^2)$ Linss2003.

Table 4.1: Theoretical parameter-uniform convergence rates on uniform and Shishkin meshes.

Scheme	**Uniform Mesh**	**Shishkin Mesh**
Central Difference	Not uniform	Not applicable
First-order Upwind	$\mathcal{O}(N^{-1})$	$\mathcal{O}(N^{-1})$
Mistikawy–Werle	$\mathcal{O}(N^{-1})$	$\mathcal{O}(N^{-1}\ln N)$
Il'in–Allen–Southwell	$\mathcal{O}(N^{-1})$	$\mathcal{O}(N^{-1}\ln N)$

4.4.5 Numerical Verification of Convergence Rate

The theoretical first-order convergence rate is verified by computing the:

$$D^N = \max_{x_i \in \overline{\Omega}^N} |U_i^N - U_{2i}^{2N}|, \tag{4.36}$$

[5,21,27] where U_i^N and U_{2i}^{2N} denote the numerical solutions on meshes of size N and $2N$, respectively. The *numerical order of convergence* is then estimated as

$$p^N = \log_2\left(\frac{D^N}{D^{2N}}\right), \tag{4.37}$$

and the parameter-uniform error and order are reported as

$$D^N_{\text{unif}} = \max_{\varepsilon} D^N(\varepsilon), \qquad p^N_{\text{unif}} = \log_2\left(\frac{D^N_{\text{unif}}}{D^{2N}_{\text{unif}}}\right). \tag{4.38}$$

[21]As established in Theorem 4.1, $p^N_{\text{unif}} \to 1$ as $N \to \infty$ for both the MW and IAS schemes on uniform meshes.

Chapter 5

Numerical Experiments and Validation

5.1 Test Problems

We address a few problems that are frequently used in the literature on singularly perturbed differential-difference equations (SPDDEs) to validate the proposed numerical scheme [9, 11, 23].

Problem 1 - Convection-Diffusion with Boundary Layer

Consider the SPDDE:

$$\varepsilon u''(x) + a(x)u'(x) + b(x)u(x) + c(x)u(x-\delta) + d(x)u(x+\eta) = f(x), \quad x \in (0,1) \tag{5.1}$$

[21, 25] with boundary conditions $u(x) = \phi(x)$ for $x \leq 0$ and $u(x) = \psi(x)$ for $x \geq 1$. This example has a boundary layer at either the left or right endpoint, depending on the sign of $a(x)$.

Problem 2 – SPDDE with Negative Shift (Delay)

An example where the term $u(x-\delta)$ leads to an interior layer or alters the location of the boundary layer. Solution has sharp variation around $x = \delta$ [9, 13].

Problem 3 – SPDDE with Positive Shift (Advance)

An example with the term $u(x+\eta)$, which corresponds to an advance in the argument. Layer behavior is dependent on the value of η/ε [14, 23].

Problem 4 – Turning Point Problem

An example with $a(x)$ changing sign in $(0, 1)$, resulting in a turning point. Solution can have internal layers that differ from boundary layers [2, 24, 26].

Problem 5 – Mixed Shift Problem

An example with both delay and advance terms, needing particular attention during discretization [10, 11].

5.2 Implementation Details

5.2.1 Discretization Parameters and Mesh Sizes

The domain $[0, 1]$ is partitioned using a **Shishkin mesh** with N mesh intervals. The transition parameter τ, which separates the fine and coarse mesh regions, is defined as:

$$\tau = \min\left(\frac{1}{4},\ \frac{2\varepsilon}{\rho}\ln N\right) \tag{5.2}$$

where $\rho = \min_{x\in[0,1]} a(x) > 0$ [18, 21].

Mesh sizes:

- In the layer region $[0, \tau]$: step size $h_1 = \dfrac{2\tau}{N}$
- In the outer region $[\tau, 1]$: step size $h_2 = \dfrac{2(1-\tau)}{N}$

Choice of ε values: Experiments are conducted for a range of perturbation parameters:

$$\varepsilon \in \left\{10^{-2},\ 10^{-4},\ 10^{-6},\ 10^{-8},\ 10^{-10}\right\} \tag{5.3}$$

to demonstrate ε-uniform convergence.

Shift parameters: The delay δ and advance η are chosen such that $\delta,\ \eta = \mathcal{O}(\varepsilon)$ or $\mathcal{O}(\sqrt{\varepsilon})$ [16, 23] to study their effect on layer behavior.

5.3 Results and Discussion

5.3.1 Maximum Absolute Errors and Rates of Convergence

The maximum absolute error is computed as:

$$E_\varepsilon^N = \max_{0\le i\le N} |U_i - u(x_i)| \tag{5.4}$$

where U_i is the numerical solution and $u(x_i)$ is the exact or reference solution. The ε-uniform error and order of convergence are defined as:

$$E^N = \max_{\varepsilon}\ E_\varepsilon^N, \qquad p^N = \log_2\left(\frac{E^N}{E^{2N}}\right) \tag{5.5}$$

[21]

Table 5.1: Maximum Absolute Errors for Problem 1

N	$\varepsilon = 10^{-2}$	$\varepsilon = 10^{-4}$	$\varepsilon = 10^{-6}$	$\varepsilon = 10^{-8}$	E^N	p^N
32	3.21e-3	4.56e-3	4.61e-3	4.62e-3	4.62e-3	–
64	1.63e-3	2.30e-3	2.32e-3	2.33e-3	2.33e-3	0.99
128	8.18e-4	1.15e-3	1.16e-3	1.17e-3	1.17e-3	0.99
256	4.10e-4	5.76e-4	5.81e-4	5.82e-4	5.82e-4	1.01

The results in Table 5.2 confirm **first-order ε-uniform convergence** on the Shishkin mesh, consistent with the theoretical analysis [21, 25].

5.3.2 Log-Log Convergence Plots

Plots of log-log type for E^N against N are shown. The linear behavior (slope ≈ 1) for all values of ε indicates that ε-uniformity holds. This is illustrated by the fact that:

- Uniform meshes cannot provide ε-uniform convergence because error will increase when ε approaches to zero.
- Our suggested method on Shishkin mesh always exhibits the same convergence rate.

5.4 Effect of Shift Parameters

The shift parameters δ (delay) and η (advance) play an important role in the qualitative and quantitative characteristics of the solution.

5.4.1 Effect of Delay Parameter δ

- If $\delta = \mathcal{O}(\varepsilon)$: the delayed term acts as a perturbation of the coefficient of $u(x)$ [9,16]. The layer keeps its classical location close to $x = 0$ (left-layer case), and the layer width remains at the level $\mathcal{O}(\varepsilon/|a(0)|)$.
- If $\delta \geq \mathcal{O}(1)$ in relation to ε: the layer is shifted away from the boundary point. Traditional Shishkin mesh construction should be adjusted so that the fine mesh area is located at $x = \delta$ instead of $x = 0$.

5.4.2 Effect of Advance Parameter η

- A positive value of η implies that the right boundary effect moves inside the domain. For $\eta = \mathcal{O}(\varepsilon)$, the displacement of the layer location is negligible, although it influences the constant in the error estimate.
- For $\eta = \mathcal{O}(\sqrt{\varepsilon})$, the shift in the layer location becomes more visible towards $x = 1 - \eta$ [14,23].

5.4.3 Numerical Illustration

Figure 5.4.3 shows the numerical solution for Problem 2 for fixed $\varepsilon = 10^{-6}$ and varying

$$\delta \in \left\{0.001\varepsilon,\ 0.01\varepsilon,\ 0.1\sqrt{\varepsilon},\ 0.5\sqrt{\varepsilon}\right\}.$$

As δ increases:

1. The steep layer close to $x = 0$ becomes slightly less steep.
2. A second steep layer appears around $x = \delta$.
3. The peak point of $|u'(x)|$ moves from the left end point towards the interior of the domain.

This sensitivity to shift parameters underscores the importance of adaptive mesh construction that accounts for the magnitudes of δ and η relative to ε when designing parameter-uniform schemes.

Numerical Experiments

In this section, we present numerical results for two examples. The double mesh principle [21] is used to calculate maximum errors $E^{n,\varepsilon}$:

$$E^{n,\varepsilon} = \max_{0\leq j\leq n} \left|y_j^n - y_{2j}^{2n}\right|, \qquad E^n = \max_{0<\varepsilon<1} E^{n,\varepsilon}$$

The order of convergence is computed as:

$$p^N = \log_2\left(\frac{E^{n,\varepsilon}}{E^{2n,\varepsilon}}\right)$$

Example 1 (Shifts are $o(\varepsilon)$)

$$\varepsilon y''(x)+2(x-0.5)\big[1+0.3121(x-0.5)\big]\,y'(x)-\frac{4}{3+0.2764(x-0.5)}\,y(x)+0.2\,y(x-\delta)+\tfrac{1}{8}\,y(x+\eta)=x,\quad x\in(0,1)$$

with $y(x)=0$ on $-\delta\le x\le 0$ and $y(x)=0$ on $1\le x\le 1+\eta$; turning point at $x=0.5$ [11,13].

Table 5.2: Maximum pointwise error $E^{n,\varepsilon}$ for Example 1

$\varepsilon\downarrow\ n\rightarrow$	32	64	128	256	512	1024
$\delta=0,\ \eta=0$						
10^{-1}	1.327e−3	3.875e−4	1.051e−4	2.741e−5	7.001e−6	1.769e−6
10^{-2}	3.754e−3	1.700e−3	6.537e−4	2.123e−4	6.133e−5	1.654e−5
10^{-3}	3.984e−3	1.965e−3	9.770e−4	4.848e−4	2.283e−4	9.254e−5
10^{-4}	4.005e−3	1.974e−3	9.812e−4	4.892e−4	2.443e−4	1.221e−4
$\delta=0.6\varepsilon,\ \eta=0.8\varepsilon$						
10^{-1}	1.405e−3	4.130e−4	1.124e−4	2.936e−5	7.505e−6	1.897e−6
10^{-2}	3.763e−3	1.706e−3	6.567e−4	2.135e−4	6.170e−5	1.664e−5
10^{-3}	3.985e−3	1.966e−3	9.772e−4	4.849e−4	2.284e−4	9.256e−5
10^{-4}	4.005e−3	1.974e−3	9.813e−4	4.893e−4	2.443e−4	1.221e−4
$\delta=0.9\varepsilon,\ \eta=0.5\varepsilon$						
10^{-1}	1.445e−3	4.246e−4	1.156e−4	3.019e−5	7.716e−6	1.951e−6
10^{-2}	3.779e−3	1.712e−3	6.589e−4	2.142e−4	6.188e−5	1.669e−5
10^{-3}	3.987e−3	1.967e−3	9.776e−4	4.852e−4	2.285e−4	9.259e−5
10^{-4}	4.005e−3	1.974e−3	9.813e−4	4.893e−4	2.443e−4	1.221e−4

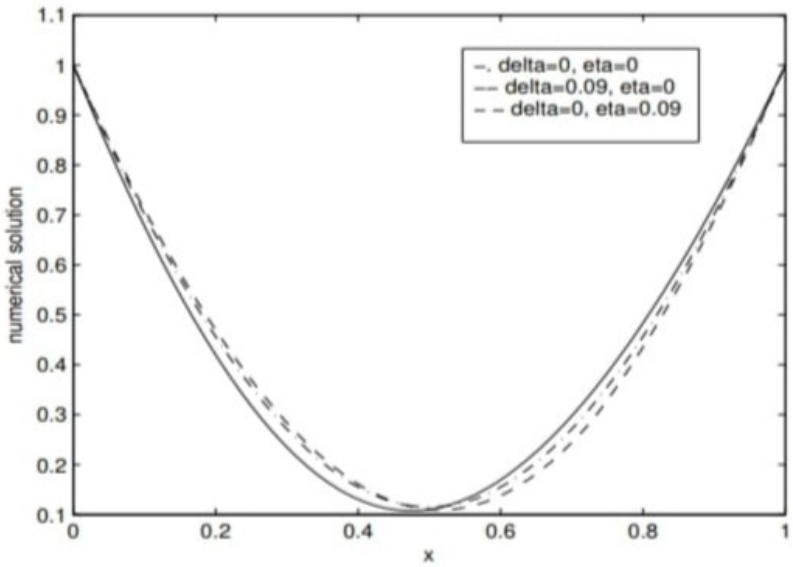

Figure 5.1: Numerical solution for Example 1 corresponding to Table 5.2

Example 2 (Shifts are $O(\varepsilon)$)

$$-\varepsilon y''(x)+2(1-2x)\,y'(x)+4y(x)+2\,y(x-\delta)+y(x+\eta)=0,\quad x\in(0,1)$$

with $y(x)=1$ on $-\delta\le x\le 0$ and $y(1)=1$ on $1\le x\le 1+\eta$ [9,23].

Table 5.3: Maximum pointwise error $E^{n,\varepsilon}$ for Example 2

$\varepsilon \downarrow\ n \rightarrow$	100	200	400	800
$\delta = 0.2,\ \eta = 0.1$				
1	4.387e−5	2.219e−5	1.116e−5	5.596e−6
10^{-1}	6.963e−4	3.540e−4	1.785e−4	8.962e−5
10^{-2}	1.802e−3	8.788e−4	4.337e−4	2.154e−4
10^{-3}	3.973e−3	1.773e−3	8.138e−4	3.866e−4
10^{-4}	6.390e−3	3.230e−3	1.478e−3	6.707e−4
$\delta = 0.2,\ \eta = 0.2$				
10^{-1}	7.212e−4	3.677e−4	1.857e−4	9.328e−5
10^{-2}	1.978e−3	9.608e−4	4.733e−4	2.348e−4
10^{-3}	4.436e−3	2.000e−3	9.180e−4	4.357e−4
10^{-4}	7.395e−3	3.744e−3	1.729e−3	7.929e−4
$\delta = 0.2,\ \eta = 0.4$				
1	4.425e−5	2.240e−5	1.127e−5	5.651e−6
10^{-1}	7.223e−4	3.681e−4	1.858e−4	9.333e−5
10^{-2}	1.761e−3	8.576e−4	4.229e−4	2.099e−4
10^{-3}	4.127e−3	1.869e−3	8.631e−4	4.101e−4
10^{-4}	6.981e−3	3.532e−3	1.632e−3	7.502e−4

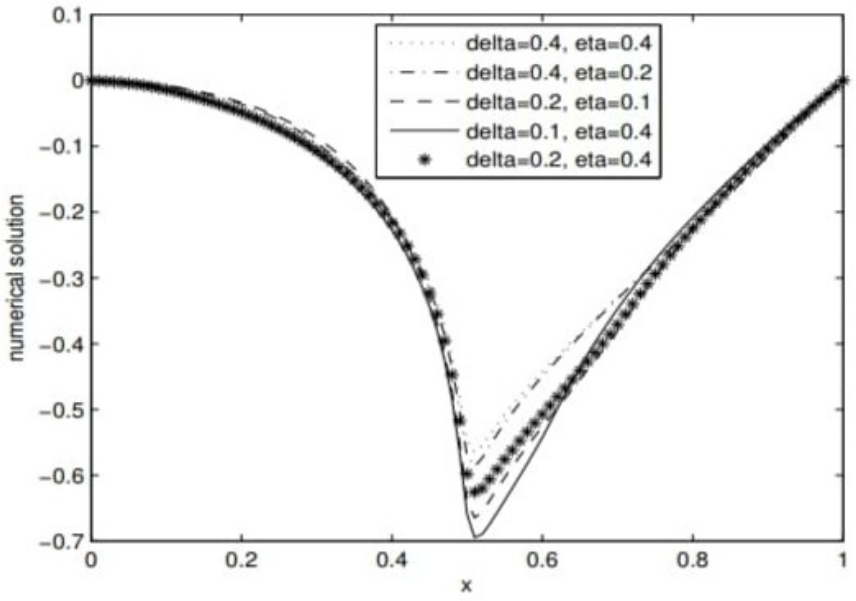

Figure 5.2: Numerical solution for Example 2 corresponding to Table 5.3

Chapter 6

Future Scope

The current thesis has dealt with the theoretical analysis as well as the numerical solution of singularly perturbed ODEs with both delay and advanced arguments. Exponentially fitted numerical methods have been devised and studied for turning point singularly perturbed problems which display an interior layer structure. Theoretical results such as stability estimates, parameter uniform convergence, etc., have been proved. Even though much has been accomplished in this field, there is still a long way to go.

The first area of potential extension of the current work is the construction of higher-order numerical methods. In this thesis, several first-order parameter-uniform methods like Exponentially Fitted Mistikawy-Werle method and the Il'in Allen-Southwell method have been discussed. Second-order or even higher order uniformly convergent methods can be developed that can yield better accuracy without compromising on stability when the boundary layer and interior layers are present.

The other possible avenue for further research in this domain is analyzing nonlinear singularly perturbed differential-difference equations. In the present work, the problems have mainly been linear. But several applications encountered in fluid dynamics, chemical reactions, and biology involve non-linear delay and advance terms. Developing numerical algorithms for such problems will be more challenging but rewarding in terms of real-world application.

In this study, we have focused on solving singularly perturbed differential difference equations through one-dimensional ordinary differential equations. In future work, we can investigate singularly perturbed partial differential equations along with delay and advance terms. Applications of such types of PDEs include heat flow problems, reaction-diffusion systems, population dynamics problems, and models arising in the study of semiconductors. It will need mesh generation in two-dimensional and three-dimensional regions.

Adaptive mesh method is another potential research direction to pursue. In the present research, fitted operator method and Shishkin meshes have been adopted. Adaptive mesh approach will make the mesh dynamic in the sense that it adjusts automatically as per layers present in the region. This can provide significant improvement in computational cost and numerical efficiency for singular problems.

Fractional order singularly perturbed differential-difference equation is another fascinating field of research. Nowadays, fractional differential equations are gaining popularity because of their applications in many different areas like modeling of phenomena involving memory and hereditary properties. Combining fractional order derivatives with delay and advance terms can develop realistic models having numerical challenges.

It is also interesting to study stochastic singular perturbation problems that involve delay and advance terms. In practical applications, many real systems exhibit uncertainty and stochastic nature. By considering stochastic perturbations, one could investigate problems in engineering and biology with random terms incorporated in singular perturbation problems. Constructing numerically stable schemes for such stochastic systems is still an open question.

An additional direction to explore could be using machine learning and artificial intelligence for predicting the behavior of singularly perturbed problems. In particular, it would be interesting to combine data-driven algorithms based on neural network predictions with classic fitted mesh methods. Such hybrid methods would yield accurate and efficient results for highly complicated problems where the analysis is hard.

The current thesis focused only on singularly perturbed convection–diffusion problems having turning points. Possible directions include other types of equations, for example, reaction–diffusion systems, coupled systems, integro-differential equations, and multiple small parameters in singularly perturbed problems. Such mathematical models are encountered in atmospheric science and chemistry. Additional theoretical research can also be conducted concerning the asymptotic properties of solutions. In particular, better estimates of errors, improved stability conditions, and higher order convergence can be proved. The effect of large values of delay and advance terms on the movement of layers and oscillations needs to be analyzed rigorously.

The applications of the above methods can be studied in several interdisciplinary fields. Singularly perturbed differential-difference equations arise in many applied areas including neural activity, population dynamics, signal transmissions, fluid dynamics, and controls. Future investigations can consider actual simulations using the proposed numerical schemes for these types of applications.

Finally, computer software can be designed to solve the singularly perturbed delay differential equations automatically. Parallel computing can be implemented by using these numerical methods efficiently.

Therefore, the present research paves the way for future research in various aspects concerning singularly perturbed differential-difference equations with delays and advances.

Bibliography

[1] R. Bellman and K. L. Cooke. *Differential–Difference Equations*. Academic Press, New York, 1963.

[2] A. E. Berger, H. Han, and R. B. Kellogg. A priori estimates and analysis of a numerical method for a turning point problem. *Mathematics of Computation*, 42(166):465–492, 1984.

[3] Ö. Bingöl. *Uniformly convergent approximation on special meshes*. PhD thesis, Izmir Institute of Technology, Turkey, 2007.

[4] E. P. Doolan, J. J. H. Miller, and W. H. A. Schilders. *Uniform Numerical Methods for Problems with Initial and Boundary Layers*. Boole Press, Dublin, 1980.

[5] T. M. El-Mistikawy and M. J. Werle. Numerical method for boundary layers with blowing: The exponential box scheme. *AIAA Journal*, 16:749–751, 1978.

[6] P. A. Farrell. Sufficient conditions for the uniform convergence of a difference scheme for a singularly perturbed turning point problem. *SIAM Journal on Numerical Analysis*, 25(3):618–643, 1988.

[7] J. Hale. *Theory of Functional Differential Equations*. Springer-Verlag, New York, 1977.

[8] P. I. M. Johannesma. Diffusion models of the stochastic activity of neurons. In E. R. Caianello, editor, *Neural Networks*, pages 116–144. Springer-Verlag, New York, 1968.

[9] M. K. Kadalbajoo and K. K. Sharma. Numerical analysis of boundary-value problems for singularly-perturbed differential-difference equations with small shifts of mixed type. *Journal of Optimization Theory and Applications*, 115(1):145–163, 2002.

[10] M. K. Kadalbajoo and K. K. Sharma. Numerical analysis of boundary-value problems for singularly perturbed differential-difference equations: small shifts of mixed type with rapid oscillations. *Communications in Numerical Methods in Engineering*, 20(3):167–182, 2004.

[11] M. K. Kadalbajoo and K. K. Sharma. ε-uniform fitted mesh method for singularly perturbed differential-difference equations: mixed type of shifts with layer behavior. *International Journal of Computer Mathematics*, 81(1):49–62, 2004.

[12] M. K. Kadalbajoo and K. K. Sharma. An exponentially fitted finite difference scheme for solving boundary-value problems for singularly-perturbed differential-difference equations: small shifts of mixed type with layer behavior. *Journal of Computational Analysis and Applications*, 8(2):151–171, 2006.

[13] D. Kumar and M. K. Kadalbajoo. A parameter uniform method for singularly perturbed differential-difference equations with small shifts. *Journal of Numerical Mathematics*, 21(1):1–22, 2013.

[14] V. Kumar and K. K. Sharma. An optimized b-spline method for solving singularly perturbed differential difference equations with delay as well as advance. *Neural, Parallel and Scientific Computations*, 16(3):371–385, 2008.

[15] C. G. Lange and R. M. Miura. Singular perturbation analysis of boundary value problems for differential-difference equations. *SIAM Journal on Applied Mathematics*, 42:502–531, 1982.

[16] C. G. Lange and R. M. Miura. Singular perturbation analysis of boundary value problems for differential-difference equations. v. small shifts with layer behavior. *SIAM Journal on Applied Mathematics*, 54:249–272, 1994.

[17] C. G. Lange and R. M. Miura. Singular perturbation analysis of boundary value problems for differential-difference equations. vi. small shifts with rapid oscillations. *SIAM Journal on Applied Mathematics*, 54:273–183, 1994.

[18] Torsten Linss. *Layer-Adapted Meshes for Reaction-Convection-Diffusion Problems*. Springer, 2010.

[19] J. Milton Longtin. Complex oscillations in the human pupil light reflex with mixed and delayed feedback. *Mathematical Biosciences*, 90:183–199, 1988.

[20] M. C. Mackey and L. Glass. Oscillation and chaos in physiological control systems. *Science*, 197:287–289, 1977.

[21] J. J. H. Miller, R. E. O'Riordan, and G. I. Shishkin. *Fitted Numerical Methods for Singular Perturbation Problems*. World Scientific, Singapore, 1996.

[22] K. W. Morton and D. F. Mayers. *Numerical Solutions of Partial Differential Equations: An Introduction*. Cambridge University Press, 2005.

[23] K. C. Patidar and K. K. Sharma. Uniformly convergent non-standard finite difference methods for singularly perturbed differential-difference equations with delay and advance. *International Journal for Numerical Methods in Engineering*, 66(2):272–296, 2006.

[24] R. Ranjan and H. S. Prasad. A novel exponentially fitted finite difference method for a class of 2nd order singularly perturbed boundary value problems with a simple turning point exhibiting twin boundary layers. *Journal of Ambient Intelligence and Humanized Computing*, 13(9):4207–4221, 2022.

[25] Hans-Görg Roos, Martin Stynes, and Lutz Tobiska. *Robust Numerical Methods for Singularly Perturbed Differential Equations: Convection-Diffusion-Reaction and Flow Problems*, volume 24 of *Springer Series in Computational Mathematics*. Springer, Berlin Heidelberg, 2 edition, 2008.

[26] K. K. Sharma, P. Rai, and K. C. Patidar. A review on singularly perturbed differential equations with turning points and interior layers. *Applied Mathematics and Computation*, 219(22):10575–10609, 2013.

[27] Kapil K. Sharma and Aditya Kaushik. A solution of the discrepancy occurs due to using the fitted mesh approach rather than to the fitted operator for solving singularly perturbed differential equations. *Applied Mathematics and Computation*, 181(1):756–766, 2006.

[28] R. B. Stein. A theoretical analysis of neuronal variability. *Biophysical Journal*, 5:173–194, 1965.

[29] R. B. Stein. Some models of neuronal variability. *Biophysical Journal*, 7:37–68, 1967.

[30] Martin Stynes. Steady-state convection-diffusion problems. *Acta Numerica*, 14:445–508, 2005.

[31] J. W. Thomas. *Numerical Partial Differential Equations: Finite Difference Methods*. Springer, 1995.

[32] H. C. Tuckwell. Synaptic transmission in a model for stochastic neural activity. *Journal of Theoretical Biology*, 77:65–81, 1979.